# Optimal angle bounds for Steiner triangulations of polygons

Christopher J. Bishop \*

#### Abstract

For any simple polygon P we compute the optimal upper and lower angle bounds for triangulating P with Steiner points, and show that these bounds can be attained (except in one special case). The sharp angle bounds for an N-gon are computable in time O(N), even though the number of triangles needed to attain these bounds has no bound in terms of N alone. In general, the sharp upper and lower bounds cannot both be attained by a single triangulation, although this does happen in some cases. For example, we show that any polygon with minimal interior angle  $\theta$  has a triangulation with all angles in the interval  $I = [\theta, 90^{\circ} - \min(36^{\circ}, \theta)/2]$ , and for  $\theta \leq 36^{\circ}$  both bounds are best possible. Surprisingly, we prove the optimal angle bounds for polygonal triangulations are the same as for triangular dissections. The proof of this verifies, in a stronger form, a 1984 conjecture of Gerver.

#### 1 Statement of results

This is an announcement of results that are proven in full in [7]. Some proofs will be sketched here, but various details, especially involving estimates for conformal or quasiconformal mappings are given in [7].

It is a problem of long-standing theoretical and practical interest to triangulate a polygon with the best possible bounds on the angles used. For example, the constrained Delaunay triangulation famously maximizes the minimal angle if no additional vertices (called Steiner points) are allowed [17], [18], and algorithms for minimizing the maximum angle (again without Steiner points) are given in [3] and [13]. Here we solve the analogous problems when Steiner points are permitted.

In this case, Burago and Zalgaller [8] proved in 1960 that every planar polygon P has an acute triangulation (all angles  $< 90^{\circ}$ ). See also [2], [4], [20], [24], [29]. Since the three angles of a triangle sum to  $180^{\circ}$ , any triangle with an angle  $\le \theta$ , must have an angle  $\ge 90^{\circ} - \theta/2$ . It follows that  $90^{\circ}$  is the smallest upper bound that holds uniformly for all polygons, but what are the optimal upper and lower angle bounds for triangulating a given polygon P with Steiner points? Are these bounds attained or can they only be approximated? Can both bounds be attained simultaneously? How do the angle bounds for triangulations differ from those for dissections? Using ideas involving conformal and quasiconformal mappings, we shall answer each of these questions. Our emphasis is on computing the optimal angle bounds and showing they are attained by some triangulation; finding such triangulations with (nearly) the optimal number of elements remains an interesting open question.

We start with some notation. Suppose  $\mathcal{T}$  is a triangulation of P. Let  $V_P$  be the vertex set of P,  $V_{\mathcal{T}}$  the vertex set of  $\mathcal{T}$ ,  $\partial \mathcal{T} = V_{\mathcal{T}} \cap P$  the **boundary vertices** of  $\mathcal{T}$ , and let  $\operatorname{int}(\mathcal{T}) = V_{\mathcal{T}} \setminus \partial \mathcal{T}$  denote the **interior vertices**. For  $v \in V_{\mathcal{T}}$ , let L(v) be the number of triangles in  $\mathcal{T}$  that have v as a vertex. For  $v \in \partial \mathcal{T}$ , we define its **discrete curvature** as  $\kappa(v) = 3 - L(v)$ , and for an interior vertex we set  $\kappa(v) = 6 - L(v)$ . Using these definitions, Euler's formula applied to a triangulation can be rewritten to look like the Gauss-Bonnet formula:

(1.1) 
$$\sum_{v \in \text{int}(\mathcal{T})} \kappa(v) = 6 - \sum_{v \in \partial \mathcal{T}} \kappa(v).$$

This common value is denoted  $\kappa(\mathcal{T})$ , the curvature of the triangulation.

For  $\phi > 0$ , a  $\phi$ -triangulation of P is one with all angles  $\leq \phi$ . For  $\phi \in [60^{\circ}, 90^{\circ}]$  define the interval  $I(\phi) = [180 - 2\phi, \phi]$ . Any  $\phi$ -triangulation must have all of its angles in  $I(\phi)$  (since the sum of all three angles is  $180^{\circ}$ , if two are  $\leq \phi$ , the third is  $\geq 180^{\circ} - 2\phi$ ). Let  $|V_P|$  be the number of vertices in P, and for  $v \in V_P$ , let  $\theta_v$ 

<sup>\*</sup>The author is partially supported by NSF Grant DMS 1906259.

<sup>&</sup>lt;sup>1</sup>The full version of the paper can be accessed at http://www.math.stonybrook.edu/~bishop/papers/soda22\_long.pdf

denote the interior angle of P at v. A labeling  $L: V_P \to \mathbb{N} = \{1, 2, ...\}$  is called  $\phi$ -admissible if  $\theta_v \in L(v) \cdot I(\phi)$  for every  $v \in V_P$ . The curvature of a labeling L is defined as

$$\kappa(L) = \sum_{v \in V_P} L(v) - (3|V_P| - 6) = 6 - \sum_{v \in V_P} (3 - L(v)).$$

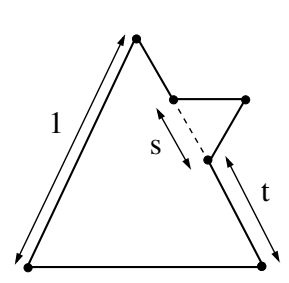
If a labeling L of  $V_P$  comes from a  $\phi$ -triangulation  $\mathcal{T}$  of P with  $\phi < 90^\circ$ , then it is automatically  $\phi$ -admissible and satisfies  $\kappa(L) \leq \kappa(\mathcal{T})$ , since vertices of  $\partial \mathcal{T} \setminus V_P$  must have degree  $\geq 3$ . If  $\phi < 72^\circ$  then int( $\mathcal{T}$ ) has no vertices of degree  $\leq 5$ , so (1.1) implies  $\kappa(L) \leq \kappa(\mathcal{T}) \leq 0$ . See Figure 1. Similarly, if  $\phi < \frac{5}{7} \cdot 90^\circ \approx 64.2857^\circ$  then every vertex in int( $\mathcal{T}$ ) has degree 6 and every vertex in  $\partial \mathcal{T} \setminus V_P$  has degree 3, so  $\kappa(L) = \kappa(\mathcal{T}) = 0$ . Remarkably, these elementary necessary conditions are also sufficient.

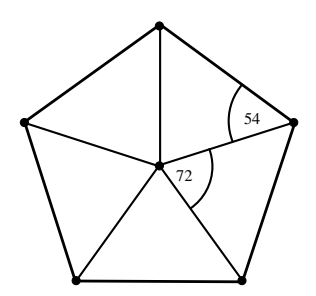
Theorem 1.1. For  $60^{\circ} < \phi \leq 90^{\circ}$ , a polygon P has a  $\phi$ -triangulation iff

- 1.  $72^{\circ} \leq \phi < 90^{\circ}$  and there is some  $\phi$ -admissible labeling L of  $V_P$ ,
- 2.  $\frac{5}{7} \cdot 90^{\circ} < \phi < 72^{\circ}$ , and there is a  $\phi$ -admissible labeling with  $\kappa(L) \leq 0$ ,
- 3.  $60^{\circ} < \phi < \frac{5}{7} \cdot 90^{\circ}$ , and there is a  $\phi$ -admissible labeling with  $\kappa(L) = 0$ .

For  $60^{\circ} < \phi < 90^{\circ}$  define  $\mathcal{K}(\phi)$  be the set of possible values of  $\kappa(L)$  over all  $\phi$ -admissible labelings of  $V_P$ ; we set  $\mathcal{K}(\phi) = \infty$  if there is no admissible labeling. Note that  $\mathcal{K}(\phi)$  is either  $\infty$  or a non-empty interval of integers. Hence  $\mathcal{K}(\phi)$  has a unique closest element to 0, denoted  $\kappa(\phi)$  (possibly 0 or  $\infty$ ). The three conditions in Theorem 1.1 can be restated as  $\kappa(\phi) < \infty$ ,  $\kappa(\phi) \leq 0$  and  $\kappa(\phi) = 0$  respectively. (We should write  $\mathcal{K}(\phi, P)$ ,  $\kappa(\phi, P)$ , since these quantities also depend on P, but in this paper P is usually fixed and clear from context.)

Figure 1 shows that a polygon can satisfy  $\kappa(60^\circ) = 0$ , but have no equilateral triangulation. Thus Theorem 1.1 fails for  $\phi = 60^\circ$ . Note that  $\kappa(60^\circ) = 0$  if and only if P is a  $60^\circ$ -polygon, i.e., all angles are multiples of  $60^\circ$ . Such a polygon has an equilateral triangulation iff all of its edge lengths are integer multiples of a single value. However, if  $\kappa(60^\circ) = 0$ , then P can always be triangulated using only angles  $\leq 60^\circ + \epsilon$  for any  $\epsilon > 0$ ; see Lemma 3.5. This is the only case where the optimal bound need not be attained by any triangulation.





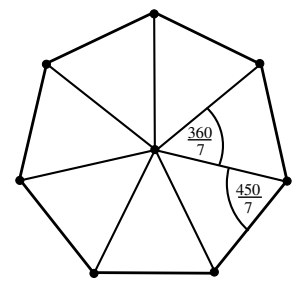


Figure 1: The left polygon satisfies  $\kappa(60^{\circ}) = 0$ , but has no equilateral triangulation unless both s and t are rational. The other pictures show where the special angles in Theorem 1.1 come from: these angles are forced by interior vertices of degree five or seven.

For a simple polygon P, and let  $\theta_{\min}$  and  $\theta_{\max}$  denote the minimum and maximum interior angles of P and define  $\Phi(P)$  to be the infimum of  $\phi$  such that P has a  $\phi$ -triangulation. The proofs of the following consequences of Theorem 1.1 may be found in [7].

COROLLARY 1.1.  $\Phi(P)$  can be computed in time  $O(|V_P|)$ .

COROLLARY 1.2. For any polygon,  $\Phi(P) \leq 90^{\circ} - \min(\theta_{\min}, 36^{\circ})/2$ , with equality if  $\theta_{\min} \leq 36^{\circ}$ .

COROLLARY 1.3. For the regular N-gon  $P_N$ ,  $\Phi(P_N) = 72^{\circ}$  except when N = 3, 6, 7, 8, 9; then  $\Phi(P_N) = 60^{\circ}$ ,  $60^{\circ}$ ,  $\frac{5}{7} \cdot 90^{\circ}$ ,  $67.5^{\circ}$ , and  $70^{\circ}$  respectively.

A **triangular dissection** covers P and its interior by finitely many closed triangles with disjoint interiors. The edges of adjacent triangles need not match up; if they do, then we have a triangulation. See Figure 2. A  $\phi$ -dissection is a triangular dissection with all angles  $\leq \phi$ . In 1984 Gerver [15] showed that the conditions in Theorem 1.1 are necessary if P has a  $(\phi + \epsilon)$ -dissection for every  $\epsilon > 0$ , and he conjectured that they were sufficient for a  $\phi$ -dissection to exist if  $\phi > 60^{\circ}$ . Theorem 1.1 strengthens this by proving that a  $\phi$ -triangulation exists.

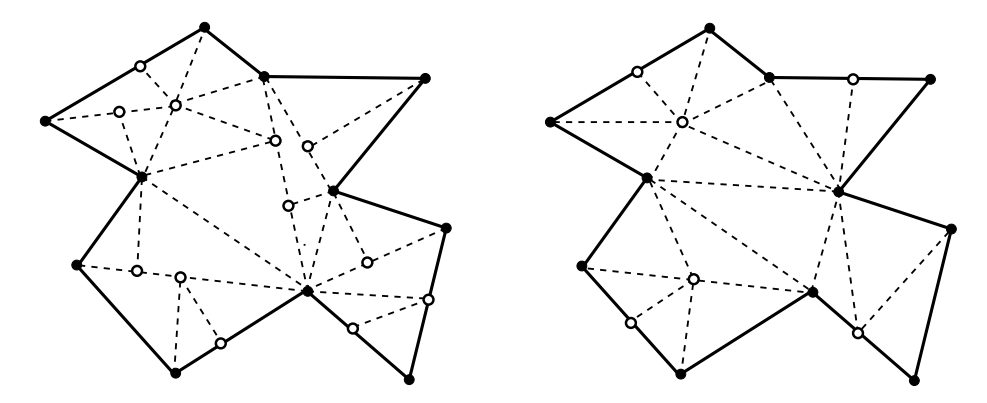


Figure 2: On the left is a dissection of a polygon and on the right a triangulation. The white dots the Steiner points. Despite triangulations being more restrictive than dissections, the optimal upper angle bounds are the same for both types of decomposition.

COROLLARY 1.4. For a polygon P and  $\phi \in (60^{\circ}, 90^{\circ}]$ , the following are equivalent:

- 1. For every  $\epsilon > 0$ , P has a  $(\phi + \epsilon)$ -dissection,
- 2. P has a  $\phi$ -dissection,
- 3. P has a  $\phi$ -triangulation.

The conditions in Theorem 1.1 only depend on the set of angles of P, not on their ordering around P, nor on the side lengths of P. This solves Problem C7 of [10].

COROLLARY 1.5. If  $\phi > 60^{\circ}$  and P, P' are N-gons with the same set of angles (possibly in different orders around the boundary) then P has a  $\phi$ -triangulation (or a  $\phi$ -dissection) if and only if P' does.

As noted earlier, the constrained Delaunay triangulation maximizes the minimal angle needed for polygonal triangulations without Steiner points (see [17], [18]), and an algorithm using only interior Steiner points is presented in [21]. The methods of this paper can be used to maximize the minimum angle for triangulating a polygon P with arbitrary Steiner points. To see how this works, suppose  $0 < \phi < 60^{\circ}$  and define  $\tilde{I}(\phi) = [\phi, 180^{\circ} - 2\phi]$ ; similar to the argument given for  $I(\phi)$ , any triangle having smallest angle  $\phi$  must have all its angles inside  $\tilde{I}(\phi)$ . Define a labeling L to be  $\phi$ -lower-admissible if  $\theta_v \in L(v) \cdot \tilde{I}(\phi)$  where  $\theta_v$  is the angle of P at  $v \in V_P$ . The curvature  $\kappa(L)$  is defined just as before, and  $\tilde{K}(\phi)$  is the set of curvatures of  $\phi$ -lower-admissible labelings. Also as before,  $\tilde{\kappa}(\phi)$  is the element of this set closest to 0 (equal to  $\infty$  if no  $\phi$ -lower-admissible labeling exists). A  $\phi$ -lower-triangulation is a triangulation with all angles  $\geq \phi$ . We define  $\tilde{\Phi}(P)$  to be the supremum of  $\phi$  so that P has a  $\phi$ -lower-triangulation.

Theorem 1.2. For  $0 < \phi < 60^{\circ}$ , a polygon P has a  $\phi$ -lower-triangulation iff

- 1.  $0 < \phi \le \frac{1}{7} \cdot 360^{\circ} \approx 51.4286^{\circ}$  and  $\widetilde{\kappa}(\phi) < \infty$ ,
- 2.  $\frac{1}{7} \cdot 360^{\circ} < \phi \leq 54^{\circ}$ , and  $\widetilde{\kappa}(\phi) \geq 0$ ,
- 3.  $54^{\circ} < \phi < 60^{\circ}$ , and  $\widetilde{\kappa}(\phi) = 0$ .

As before, there are a variety of consequences that follow; these are proven in [7].

COROLLARY 1.6.  $\widetilde{\Phi}(P)$  can be computed in time  $O(|V_P|)$ .

COROLLARY 1.7. If P has a  $\phi$ -lower-triangulation then it also has an acute  $\phi$ -lower-triangulation.

COROLLARY 1.8. If  $\theta_{\min} \leq 45^{\circ}$ , then  $\widetilde{\Phi}(P) = \theta_{\min}$ .

Using Corollaries 1.2 and 1.8, we see that if P is a polygon with  $\theta_{\min} = 45^{\circ}$ , then  $\Phi(P) \leq 72^{\circ}$  and  $\widetilde{\Phi}(P) \geq 45^{\circ}$ . If P has at least one angle  $\theta \in (72^{\circ}, 90^{\circ})$ , then any triangulation of P that attains the optimal upper bound  $\Phi(P)$  must subdivide  $\theta$  and hence has an angle strictly less than  $45^{\circ} \leq \widetilde{\Phi}(\phi)$ .

COROLLARY 1.9. There exist polygons so that any triangulation attaining the optimal upper angle bound  $\Phi(P)$ , does not achieve the optimal lower angle bound  $\widetilde{\Phi}(P)$ .

The idea behind both Theorems 1.1 and 1.2 is to associate to each polygon P a 60°-polygon P', and then to transfer a nearly equilateral triangulation from P' to P using a conformal map. We map the triangulation vertices from P' to P and connect them by segments in P; we call these the "pushed forward" triangles (conformal images of the triangles themselves would have curved sides). A simple example is shown in Figure 3. The labeling shown in Figure 3 is 72°-admissible and has curvature 0, so  $\kappa(72^\circ) = 0$ . Moreover, the reader can check that  $\kappa(\phi) > 0$  for  $\phi < 72^\circ$ , hence  $\Phi(P) = 72^\circ$ .

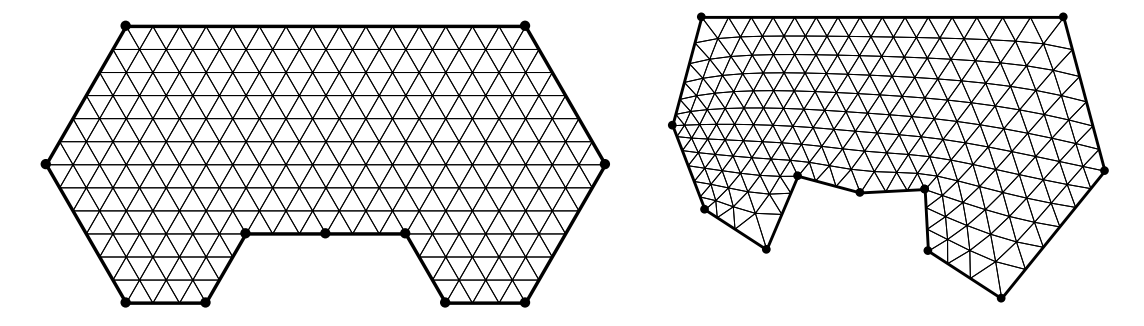


Figure 3: An equilateral triangulation of P' (left) and its conformal image P (angles: 270°, 126°, 96°, 126°, 105°, 105°, 144°, 144°, 80°, 262°, 162°). The maximum angle is  $\approx 73.5205^{\circ}$  and approaches 72° as the mesh gets finer; 72° is sharp and can be attained by modifying a sufficiently fine triangulation near the vertices.

Note that any nearly equilateral triangulation of a polygon has all interior vertices of degree six, and hence has curvature zero. If P' is a  $60^{\circ}$ -polygon associated to a polygon P, then the angle of P' at the vertex v' corresponding to  $v \in V_P$  is given by  $60^{\circ} \cdot L(v)$ , where L is a labeling of  $V_P$ . Since the angles of P' sum to  $(|V_P|-2) \cdot 180^{\circ}$ , a short calculation shows that we must have  $\kappa(L)=0$ . Conversely, given such a labeling of  $V_P$ , we will use the Schwarz-Christoffel formula to define P' and a conformal map  $f:P'\to P$ . If we transfer a sufficiently fine and nearly equilateral triangulation from P' to P using f, the image will be close to a  $\phi$ -triangulation of P if the labeling L is  $\phi$ -admissible. So to start the construction it seems that we need a  $\phi$ -admissible labeling of P with zero curvature.

However, such a labeling need not exist. For example, suppose P is a pentagon with five equal angles of  $108^{\circ}$ . Theorem 1.1 (in particular, Corollaries 1.3 and 1.5) implies that  $\Phi(P) = 72^{\circ}$ . However, the only  $72^{\circ}$ -admissible labels for a  $108^{\circ}$ -vertex are  $\{2,3\}$ , so  $\mathcal{K}(\phi) = \{1,\ldots,6\}$  and so  $\kappa(\phi) = 1 > 0$ . This holds even if we add extra  $180^{\circ}$ -vertices to P (their possible labels are  $\{3,4,5\}$ ). Therefore, any  $72^{\circ}$ -triangulation of P has positive curvature and thus at least one interior vertex of degree five (degree < 4 implies an angle  $> 90^{\circ}$ ).

How can such a triangulation be a conformal image of a triangulation of P' that only has interior vertices of degree six? The answer is that we can choose f to conformally map the interior of P' into a subdomain of P obtained by cutting a slit in P. Two adjacent edges of P' are mapped to the two sides of the slit, and some

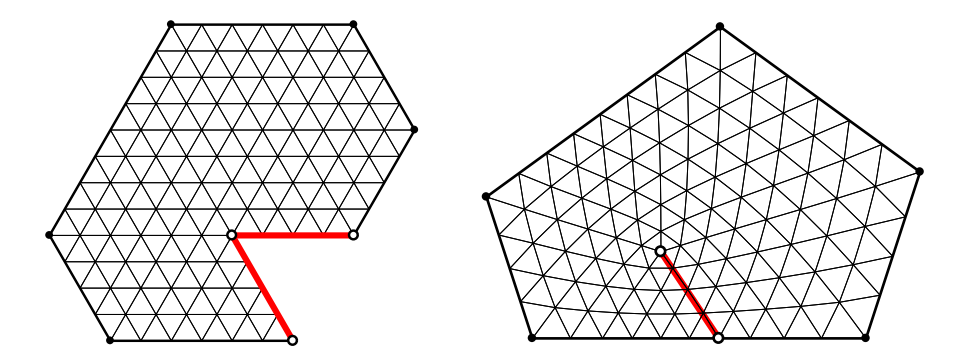


Figure 4: The edges adjacent to the  $300^{\circ}$ -vertex of P' are mapped to the two sides of the slit inside P. An interior vertex v of degree 5 is created. The slit is slightly curved to make the triangles on either side match up, although this is not easily visible (the actual slit lies slightly above the chord between its endpoints).

boundary vertices of P' become interior vertices of P, thus the topology changes. See Figure 4. In general, up to  $|\kappa(\Phi(P))|$  slits are used, introducing vertices of either degree five  $(\kappa > 0)$  or degree seven  $(\kappa < 0)$ .

This scheme encounters a number of difficulties, that we will overcome using ideas from complex function theory. We list a few here, giving details later.

- Conformal welding: When we map boundary edges of P' to a slit in P, the images of certain boundary triangles in P' must match up across the slit in P, so that the image is a triangulation and not a dissection. This is only possible if the shape of the slit is carefully chosen so that arclength on each boundary segment maps to the same measure on the slit, i.e., we need  $f(z) = f(w) \Rightarrow |f'(z)| = |f'(w)|$ . This is a special case of a conformal welding problem, e.g., [5], [16], [23], and in our case it can be solved explicitly using power maps.
- Riemann surfaces: In cases where we introduce an interior vertex of degree seven, P' will need to have a boundary vertex of degree seven, i.e., P' has interior angle 420° at some vertex. Thus we necessarily consider "polygons" P' that are actually Riemann surfaces and not planar regions. See Figure 5.

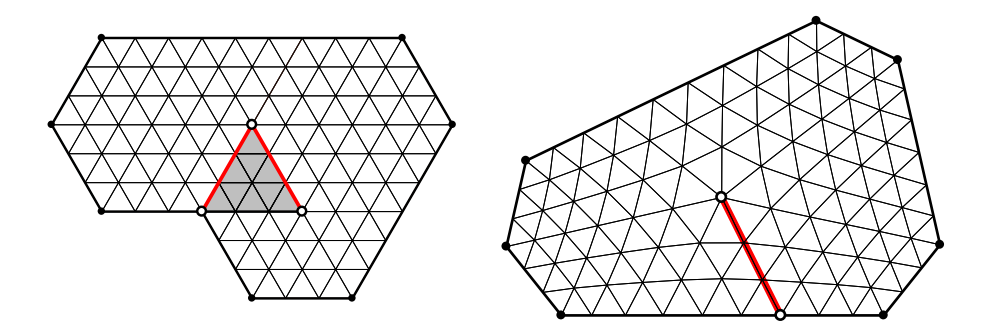


Figure 5: We triangulate an equal-angle heptagon using a Riemann surface with a 420°-vertex to insert a degree 7 vertex into the triangulation. The self-overlapping part of the surface is shaded.

- Distortion estimates: A conformal map f preserves interior angles infinitesimally, but to control our triangulation angles we shall need angle distortion estimates at positive scales, with bounds depending on the size of the triangle, its distance to the nearest vertex, and the ratio of the corresponding angles in P and P' at that vertex. Here we make use of the classical distortion theorems for conformal maps.
- Quasiconformal mappings: Given two triangulations of a region arising from different, but close, conformal maps, we merge the triangulations by using a partition of unity to interpolate from one conformal map to the other. The result is a quasiconformal map, and we shall use standard estimates on the angle distortion of such maps to control the angles of the interpolated triangulations. We also use such estimates to prove that any 60°-polygon has a nearly equilateral triangulation.

In 1992 Edelsbrunner, Tan and Waupotitsch [13] gave a  $O(N^2 \log N)$  algorithm for minimizing the maximum

angle of a polygonal triangulation without using Steiner points (their result has not been improved, so far as I know). Thus Corollary 1.1 says that it is actually faster to compute the optimal angle bound when allowing Steiner points. However a triangulation achieving the optimal bound might not be computable in polynomial time (see the remarks below), and this paper does not address the question of finding efficient triangulations attaining the optimal bounds. See the last section of [7] for some ideas on how this might be done.

Despite much effort devoted to finding triangulations with good geometry and optimal complexity, finding triangulations with optimal geometry has attracted less attention, at least when Steiner points are allowed. One case that has been considered is triangulating the square with optimal angles, a problem discussed by Gerver in [15] and by Eppstein in [14]. One possible reason that Theorem 1.1 has been overlooked is the close connection to conformal mappings; at least it is difficult to see how our proof could have been discovered using purely discrete geometric ideas. Another reason may be the traditional focus on complexity. If the size of the triangulation is bounded by a function of  $N = |V_P|$ , independent of the geometry, then 90° is the best possible upper angle bound. For example, if a  $1 \times R$  rectangle with  $R \gg 1$  is triangulated by O(1) triangles, then there must be a small angle  $\theta = O(1/R)$ , and hence some angle  $\geq 90^{\circ} - \theta/2$ . Thus the complexity of an angle-optimal triangulation of an N-gon is not polynomial in N. Even so, the sharp angle bounds proven here are fast to compute and provide a benchmark against which other triangulation methods can be compared.

Section 2 gives an overview of the proof Theorem 1.1, and later sections provide further details, assuming various estimates related to conformal and quasiconformal mappings that are proven in [7]. That paper also contains the proof of Theorem 1.2, the proof of the corollaries stated in this section, and it gives a variety of other consequences of Theorems 1.1 and 1.2. I thank Joe Mitchell and Herbert Edelsbrunner for their encouraging and helpful comments on an earlier version of this paper. I also thank the anonymous referees who read the paper for SODA 2022 and provided numerous suggestions. Several figures are drawn using Toby Driscoll's SC-Toolbox package for MATLAB [11], an improved version of an earlier algorithm of Nick Trefethen [28] for computing Schwarz-Christoffel maps. I thank Toby for his assistance with the toolbox.

#### 2 Overview of the proof

The basic idea is quite simple: we introduce a class of polygons that have "nearly equilateral" triangulations (all angles close to 60°) and use conformal maps to transfer these triangulations to general polygons.

We will say that a polygon P has **nearly equilateral triangulations** if for any  $\epsilon > 0$  it has a triangulation with all angles in  $[60^{\circ} - \epsilon, 60^{\circ} + \epsilon]$  and that each vertex of P has a neighborhood in which the triangulation elements are actually equilateral (this is needed to attain the desired angle bounds, instead of just approximating them). We will prove that every  $60^{\circ}$ -polygon has nearly equilateral triangulations; see Lemma 3.5. This lemma includes  $60^{\circ}$ -surfaces, i.e., simply connected Riemann surfaces R obtained by identifying  $60^{\circ}$ -polygons along matching edges. The boundary of R projects into the plane, possibly with self-intersections.

Suppose  $f: \Omega' \to \Omega$  is a conformal mapping between the interiors of two polygons P' and P, and that f induces a bijection between vertices of P' and vertices of P. In this paper, P' will denote a 60°-polygon (or surface) and P a general simply polygon. Below, we will often use P to refer to both the boundary curve and the interior domain, instead of using  $\Omega$  for the latter; the meaning should always be clear from context. Then f will only slightly perturb the angles of sufficiently small triangles in  $\Omega'$ , unless they are near vertices of P' (see Corollary 3.1). If v' is a vertex of P' with angle  $\psi$  that maps to a vertex v of P with angle  $\theta$ , then any small triangle close enough to v' will have its interior angles distorted by at most  $\theta/\psi$  (Lemma 3.6).

The triangulations we construct will have all their angles between 36° and 72°, except for some triangles near vertices of P that have angle less than 36°. Larger angles of P will be subdivided by the triangulation to give new angles that are all in the interval [36°, 72°], and these sub-angles should each map to 60° under the conformal map from P to P'. Thus each angle  $\theta \geq 36$ ° in P should correspond to an angle  $\psi = L(v) \cdot 60$ ° in P' that satisfies

$$\frac{5}{6}\theta \leq \psi \leq \frac{5}{3}\theta \quad \text{or equivalently} \quad \frac{\theta}{72} \leq L(v) \leq \frac{\theta}{36}.$$

For example, if P has a vertex v with interior angle  $\theta = 135^{\circ}$  the corresponding vertex v' in the 60°-polygon P' must have angle either 120° or 180°. Any other choice means that the triangles containing v' in the nearly equilateral triangulation of P' map to triangles with angles either less than 36° or larger than 72°.

Unfortunately, there are some polygons P whose vertices cannot be put into 1-1 correspondence with the vertices of a 60°-polygon so that they satisfy the restrictions in (2.2). In general, the interior angles  $\{\theta_1, \ldots, \theta_N\}$ 

of an N-gon must satisfy  $\sum_k \theta_k = (N-2)180^\circ$ . When we assign image angle values  $\{\psi_1, \dots, \psi_N\}$  using (2.2), we need to have  $\sum_k \psi_k = (N-2)180^\circ$ , but this is sometimes impossible. For example, if P is a square, then each of its four 90° angles would have to be assigned angle 120° in P', giving an angle sum  $480^\circ > 360^\circ$ . We can "fix" the angle discrepancy by adding extra vertices to the edges of P.

First suppose  $\sum_k \psi_k < \sum_k \theta_k$ . We add a new vertex v of angle 180° in an edge of P, and assign the corresponding vertex v' in P' the angle  $240^\circ \le \frac{6}{5} \cdot 180^\circ$ . See Figure 6. Doing this increases the angle sum  $\sum \theta_k$  by 180° but increases the angle sum  $\sum \psi_k$  by 240°, decreasing the gap between them by 60°. Doing this several times we can clearly make the two sums match, as desired. Four equilateral triangles in P' touch v', and they are mapped to four triangles in P touching v. These triangles have angle 45° at v and the opposite angles are approximately 67.5° (some distortion may occur). Hence using this method can only give  $\phi$ -triangulations with  $\phi \ge 67.5^\circ$ . This is adequate to prove Case 1 of Theorem 1.1 but a more elaborate construction is needed to prove Cases 2 and 3.

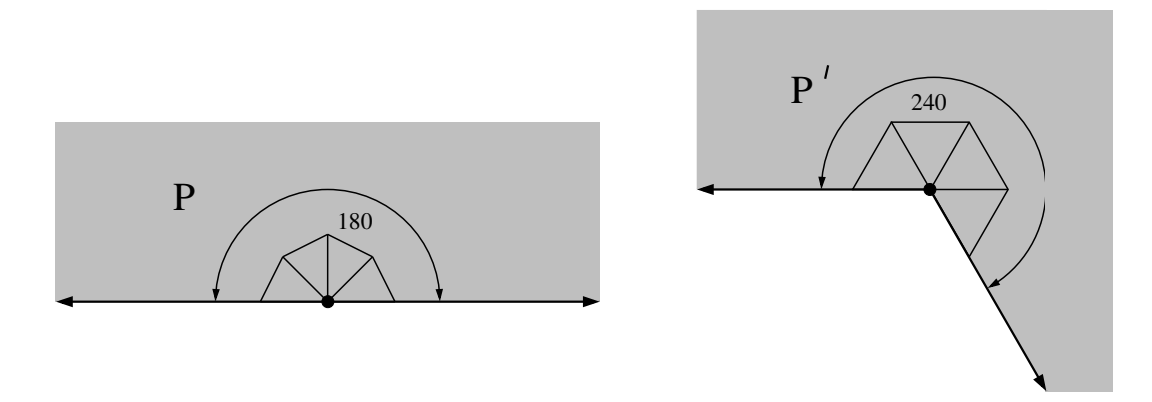
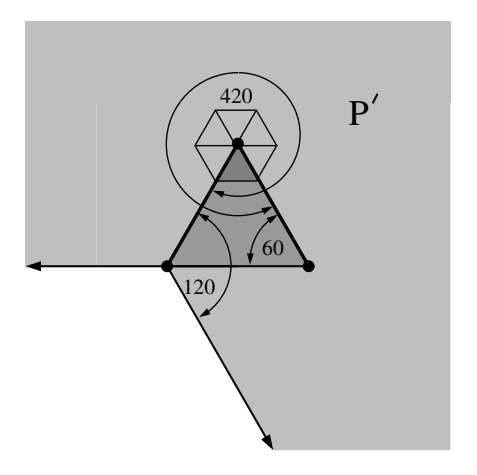


Figure 6: Our first trick for increasing the  $\psi$ -sum relative to the  $\theta$ -sum is to pair a 180°-vertex in P with a 240°-vertex in P'. The conformal map locally looks like  $z^{3/4}$ , and maps a 60° sub-angle to 45°. A triangle containing a 45° angle also contains an angle  $\geq$  67.5.

In Case 2 of Theorem 1.1 we want to decrease the angle  $67.5^{\circ}$  to  $\frac{5}{7} \cdot 90^{\circ} \approx 64.2857$ . We will do this by transferring an equilateral triangulation from a polygonal Riemann surface that has a  $420^{\circ}$  angle in its boundary. The idea is shown in Figure 7; the details will be given in Section 5. The Riemann surface R is built by attaching two planar domains as shown on the left side of Figure 13. R has a 1-1 projection onto a sector of angle  $240^{\circ}$ , except for the darker triangle where it is 2-1. Traversing the boundary, we encounter angles  $60^{\circ}$ ,  $420^{\circ}$  and  $120^{\circ}$ . The  $420^{\circ}$ -vertex belongs to seven equilateral triangles in R and will map to a degree seven interior vertex in the final triangulation.

The two segments adjacent to the 420°-vertex are mapped to a slit in P where the angles are 60°, 180° and 120°. The worst distortion comes from mapping the 420°-vertex in P' to the 360°-vertex in P (the tip of a slit). Locally the map looks like  $z^{6/7}$ , that maps each 60° sub-angle to  $\frac{6}{7} \cdot 60^\circ = \frac{4}{7} \cdot 90^\circ \approx 51.4286$ . A triangle with this angle must also contain an angle  $\geq \frac{5}{7} \cdot 90^\circ \approx 64.2857$ , which is where this angle in Theorem 1.1 comes from. Note that the two finite boundary segments of R are both mapped to the slit in P, so triangulation edges along these two sides of R must map to matching edges along the slit. Thus the conformal map must send length measure on the two segments to the same measure on the slit (but not necessarily length measure). See Figure 14.

If  $\sum_k \psi_k > \sum_k \theta_k$  we use a slightly easier variant of the 420°-trick that we call the "120°-trick". This is described in detail in Section 4. The trick involves mapping a slit half-plane to a 120°-sector with a triangle removed, as shown in Figure 8. Traversing the boundary of the slit half-plane we encounter angles 60°, 360°, and 120°, but traversing the boundary of the modified 120°-sector we encounter 60°, 300° and 120°, so the  $\psi$ -sum decreases by 60° relative to the  $\theta$ -sum. As in the 420°-trick, the shape of the slit can be chosen so that points on the two identified segments are paired according to their distance from the 300°-vertex. Then an equilateral triangulation of the modified sector maps to a triangulation of the half-plane. Note also that exactly one degree five vertex is created in the triangulation, located at the tip of the slit. See also Figure 11.



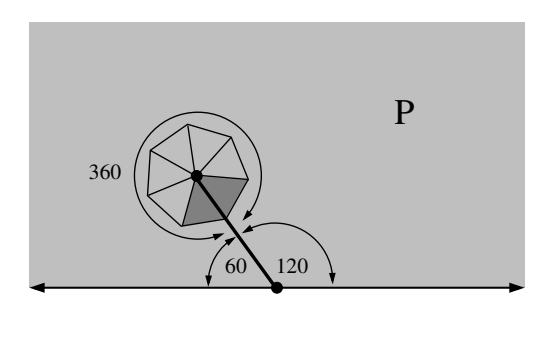


Figure 7: We cut a slit in the upper half-plane at angle  $60^{\circ}$ . This models a neighborhood of a  $180^{\circ}$ -vertex on the boundary of P. The angles we observe tracing the outline of the slit are:  $60^{\circ}$ ,  $360^{\circ}$  and  $120^{\circ}$ . The triangulation near this slit will correspond to an equilateral triangulation of a Riemann surface R with angles  $60^{\circ}$ ,  $420^{\circ}$  and  $120^{\circ}$ , pictured at right. R is a 1-1 cover of a  $240^{\circ}$ -sector, except for the darker triangle where it is 2-1.

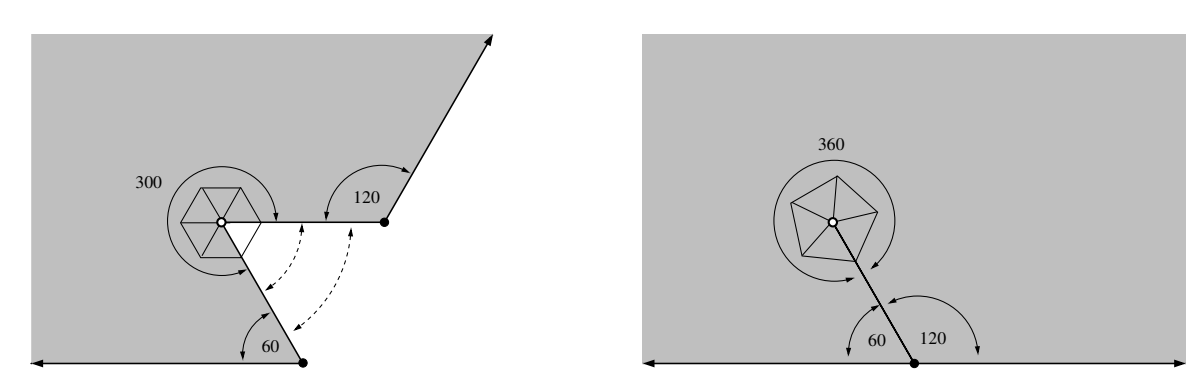


Figure 8: Take a 120°-sector and cut out an equilateral triangle (left). Conformally map this region to a slit half-plane (right). The two edges adjacent to the 300°-vertex are mapped to opposite sides of the (slightly) curved slit, and points on these edges equidistant from this vertex are identified. This implies that an equilateral triangulation on the left pushes forward to a triangulation on the right.

#### 3 Conformal and quasiconformal maps

In this section we review the definition and basic properties of conformal and quasiconformal maps and state a number of specific estimates that are used to create and merge various triangulations. Detailed proofs of all lemmas and corollaries stated here are given in [7].

We let  $D(z,r) = \{w : |z-w| < r\}$ ,  $\mathbb{D} = D(0,1)$  and  $\mathbb{T} = \partial \mathbb{D} = \{z : |z| = 1\}$ . In this paper, a **conformal** map always refers to a 1-to-1 holomorphic mapping. Thus it is angle and orientation preserving. By the Riemann mapping theorem, there is a conformal map from  $\mathbb{D}$  onto any proper, simply connected subdomain of the plane, in particular, to the interior of any bounded polygon. The conformal map is unique if we specify the image of 0 and of one boundary point. For a conformal map onto the region  $\Omega$  bounded by a N-gon P, the preimages of the N vertices are called the **conformal prevertices**. These points form an N-tuple of distinct points on  $\mathbb{T}$ . Different choices of the conformal map give N-tuples that differ by a linear fractional transformation of the disk to itself.

The Riemann mapping theorem also holds for any simply connected Riemann surface that is not conformally equivalent to the 2-sphere or the plane (this is usually called the uniformization theorem). All the Riemann surfaces that we will consider in this paper are simply connected and a have non-constant, holomorphic map into a bounded region of the plane; this implies they are conformally equivalent to the disk.

By definition, a conformal map f on a domain  $\Omega$  preserves angles infinitesimally. When we map a triangulation by a conformal map, we will not just take the image f(T) of each triangle T; this would have curved sides. If  $T = \Delta ABC \subset \Omega$  has vertices A, B, C, we define the **pushed forward triangle**  $f^*(T) = \Delta f(A)f(B)f(C)$ , i.e., the triangle with vertices f(A), f(B), f(C). See Figure 9.

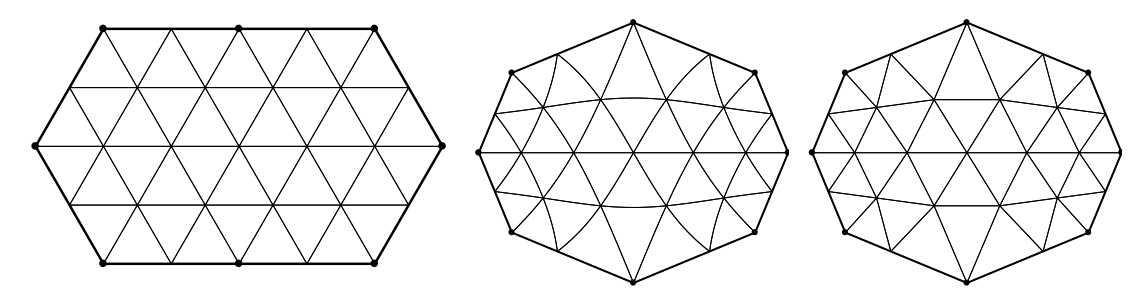


Figure 9: An equilateral triangulation (left), the actual conformal images of the triangles (center), and the pushed forward triangles (right) where vertex images are connected by segments.

LEMMA 3.1. If f is a conformal map on a disk D(z,r),  $\delta > 0$  is sufficiently small, and  $T = \Delta ABC$  is triangle inside  $D(z,\delta r)$ , then the triangle  $f^*T = \Delta f(A)f(B)f(C)$  has angles that are within  $O(\delta)$  of the corresponding angles of T.

This result allows us to quantify the fact that, except near the corners, a conformal map between polygons alters the angles of small triangles very little under the push forward operation.

COROLLARY 3.1. Suppose f is conformal map between the interiors of two polygons P and P' that maps vertices to vertices. Suppose  $V_P$  is the vertex set of P,  $\Omega$  is the interior of P, and that  $\{D_v\}_{v \in V_P}$  are disjoint disks around each vertex v. Define  $\Omega_0 = \Omega \setminus \bigcup_{v \in V_P} D_v$  and suppose  $T \subset \Omega_0$  is a triangle. Then for every  $\epsilon > 0$  there is a  $\delta > 0$  so that f changes the angles of T by less than  $\epsilon$  if  $\operatorname{diam}(T) < \delta$ .

A quasiconformal map h of the plane is a homeomorphism of the plane to itself that is absolutely continuous on almost all lines and whose **complex dilatation**  $\mu = h_{\overline{z}}/h_z$  satisfies  $\|\mu\|_{\infty} < 1$ ; recall  $h_z = \frac{1}{2}(\frac{\partial h}{\partial x} - i\frac{\partial h}{\partial y})$  and  $h_{\overline{z}} = \frac{1}{2}(\frac{\partial h}{\partial x} + i\frac{\partial h}{\partial y})$ . See [1] or [19] for the basic properties of such maps. One important such property is that pre or post composing a K-quasiconformal map by a conformal map gives another K-quasiconformal map: a simple calculation with the chain rule shows the phase of the dilatation may change, but its absolute value does not. A quasiconformal map h is called K-quasiconformal if  $\|\mu\|_{\infty} \le k = (K-1)/(K+1)$ . More geometrically, at almost every point h is differentiable and its derivative (which is a real linear map) send circles to ellipses of eccentricity at most K (the **eccentricity** of an ellipse is the ratio of the major to minor axis). An important property of K-quasiconformal maps  $\mathbb{C} \to \mathbb{C}$  is that they form a compact family when normalized to fix two points, usually taken to be 0 and 1. Also, a 1-quasiconformal map is conformal, so a 1-quasiconformal map of the plane to itself must be linear. These facts imply the following standard result.

LEMMA 3.2. For any  $\delta > 0$ , there is a  $\epsilon > 0$  so that if f is a  $(1 + \epsilon)$ -quasiconformal map from  $\{|z| < 1/\epsilon\}$  into  $\mathbb{C}$ , then  $|f(z) - z| \le \delta |f(0) - f(1)|$  on  $\mathbb{D}$ .

From this one can deduce that, like conformal maps, quasiconformal maps will not greatly distort the angles of pushed forward triangles if  $\epsilon$  is chosen small enough.

An **infinite sector** is a region congruent to  $S(\theta) = \{re^{\phi} : r > 0, -\theta/2 < \phi < \theta/2\}$ . The boundary consists of two infinite rays meeting at its vertex and the angle of the sector is the interior angle  $\theta$  made by these rays. A **finite sector** is a region congruent to  $S(\theta) \cap D(0,t)$  for some t > 0 and  $\theta \in (0,360^{\circ}]$ . For r > 1, let  $A(r) = \{z : 1/r < |z| < r\}$ . An **annular sector** is a region congruent to  $S(\theta,r) = S(\theta) \cap A(r)$ .

LEMMA 3.3. Suppose  $\Omega_1, \Omega_2$  are simply connected domains and that both  $\Omega_1 \cap A(3)$  and  $\Omega_2 \cap A(3)$  have connected components equal to  $S(\theta, 3)$ . Suppose  $f_k$  is conformal on  $\Omega_k$ , k = 1, 2 and  $\sup_{S(\theta, 3)} |f_1 - f_2| < \epsilon$ . Suppose that

 $f_1, f_2$  both map each radial segment of  $\partial S(\theta, 3)$  into the same line. Let  $\eta : [0, \infty) \to [0, 1]$  be smooth with  $\eta(r) = 0$  if r < 1/2 and  $\eta(r) = 1$  if r > 2. Then

$$g(z) = f_1(z)(1 - \eta(|z|)) + f_2(z)\eta(|z|)$$

is quasiconformal on  $\Omega_1 \cup \Omega_2$  with complex dilatation bounded by  $O(\epsilon)$ .

A similar argument also proves the following slightly simpler variation, where we assume the maps are defined on a common disk, instead of a sector. This version will be used to merge triangulations near tips of slits in the  $120^{\circ}$ -trick (see Section 4) and the  $420^{\circ}$ -trick (see Section 4).

LEMMA 3.4. Suppose  $\Omega_1, \Omega_2$  are simply connected domains and  $D(0,r) \subset \Omega_1 \cap \Omega_2$  for some r > 4. Suppose  $f: \Omega_1 \to \Omega_2$  is conformal and f(0) = 0, f'(0) = 1. Let  $\eta: [0, \infty) \to [0, 1]$  be smooth with  $\eta(r) = 0$  if  $r \le 1/2$  and = 1 if  $r \ge 2$ . Then

$$g(z) = z(1 - \eta(|z|)) + f(z)\eta(|z|)$$

is quasiconformal on  $\Omega_1 \cup \Omega_2$  with complex dilatation bounded by O(1/r).

As noted in the introduction, not every  $60^{\circ}$ -polygon P has an equilateral triangulation, but they all have nearly equilateral triangulations. Recall that this means that for any  $\epsilon > 0$ , there is a triangulation of P with all angles within  $\epsilon$  of  $60^{\circ}$  and that all angles are equal to  $60^{\circ}$  in some neighborhood of each vertex (the neighborhood may depend on the triangulation).

Lemma 3.5. Every  $60^{\circ}$ -surface P has nearly equilateral triangulations.

Roughly speaking, the proof is to explicitly construct a  $60^{\circ}$ -surface R' that has an equilateral triangulation and that closely approximates R. Then show that the conformal map  $R' \to \mathbb{D}$  can be composed with a quasiconformal map  $\mathbb{D} \to \mathbb{D}$  with small dilatation, so that the vertices of R' map to the conformal prevertices of R on  $\mathbb{T}$ . From this we get a quasiconformal map  $R' \to R$  that sends vertices to vertices and has small dilatation. Hence the equilateral triangulation of R' is pushed forward to a nearly equilateral triangulation of R (some extra work is needed to get true equilateral triangles near each vertex of R). For details see [7].

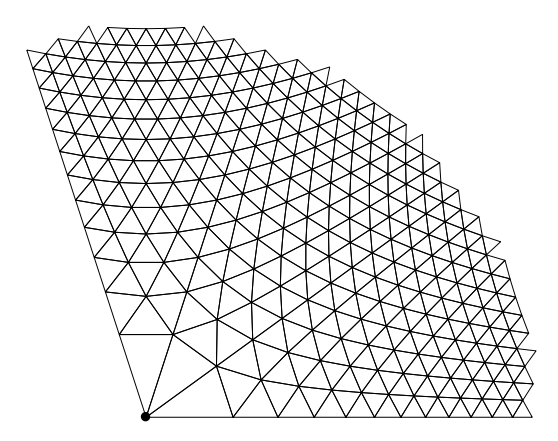
Our last application of conformal mappings is to find good triangulations of infinite sectors; these will be used to triangulate a polygon near each of its vertices. As before,  $S(\theta)$  denotes the infinite sector of angle  $\theta$  with positive real half-line as its axis of symmetry. Note that  $S(60^{\circ})$  comes with a natural equilateral triangulation  $\mathcal{G}$ . This triangulation can obviously be extended to a triangulation of the right half-plane, and our triangulations of general sectors are constructed by taking images of equilateral triangulations of special sectors (multiplies of  $60^{\circ}$ ) under power maps  $z \to z^{\alpha}$ . See Figure 10 for two examples.

LEMMA 3.6. Consider the grid  $\mathcal{G}$  of unit equilateral triangles in  $S(60^{\circ})$ . Let  $0 < \alpha \leq 2$ . Suppose  $T = \Delta ABC \in \mathcal{G}$  and  $f^*T = \Delta f(A)f(B)f(C)$ , where f is a branch of  $z^{\alpha}$  defined on T. Then the interior angles of  $f^*T$  differ from the corresponding angles of T by at most  $|\alpha - 1| \cdot \theta$  where  $\theta$  is the angle subtended by T from the origin.

COROLLARY 3.2. Suppose  $0 < \phi < 90^{\circ}$ . The sector  $S(\phi)$  has a triangulation with all angles in  $[180^{\circ} - 2\phi, \phi]$  if  $\phi \ge 60^{\circ}$ , and in  $[\phi, 90^{\circ} - \phi/2]$  if  $\phi < 60^{\circ}$ .

The sector triangulations described above are used in a neighborhood of each vertex of P. Outside these neighborhoods, the conformal image of a nearly equilateral triangulation is used. Quasiconformal interpolation is applied to merge the various triangulations in an annulus around each vertex. The precise statement of this procedure is given by the following lemma.

LEMMA 3.7. Suppose  $f: P' \to P$  is a conformal map between polygons that maps vertices to vertices. Suppose f(v') = v where v' is a vertex of P' and v is a vertex of P, with angles  $\psi = k \cdot 60^{\circ}$  and  $\theta$  respectively. Suppose  $\mathcal{T}$  is a nearly equilateral triangulation of P' and  $f^*\mathcal{T}$  the image triangulation. If  $\mathcal{T}$  is fine enough, then there is a neighborhood U of v and a triangulation  $\mathcal{S}$  of P that equals  $f^*\mathcal{T}$  outside U and every triangle of  $\mathcal{S}$  touching U has all angles bounded by  $\max(\theta/k, 90^{\circ} - \theta/2k)$ .



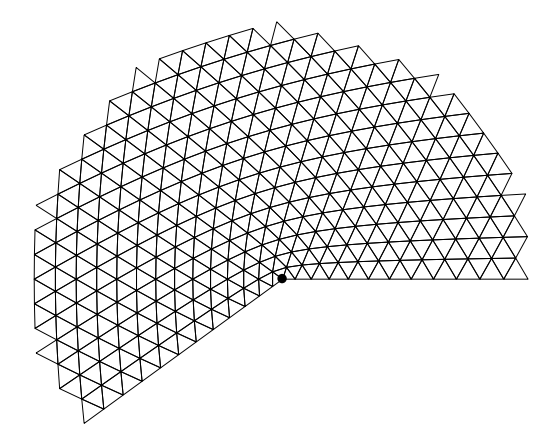


Figure 10: Image of the equilateral grid in the upper halfplane under the maps  $z^{3/5}$  and  $z^{6/5}$ . These are the extreme values that keep images of  $60^{\circ}$  angles between  $36^{\circ}$  and  $72^{\circ}$ .

#### 4 The $120^{\circ}$ -trick

In this section we provide the details of the "120°-trick" for triangulating the upper half-plane in a way that uses maximum angle 72°, and near infinity looks like the push forward under  $z^{3/2}$  of the standard equilateral mesh of a 120°-sector. This involves cutting a slit in P, as discussed in Sections 1 and 2.

Consider the region  $\Omega$  shown on the left in Figure 8. This is a 120°-sector with an equilateral triangle at the origin removed. We translate the picture so the 300°-vertex is at the origin. If we then apply a branch of  $z^{6/5}$ , the 300° angle becomes 360°, and the two finite segments in  $\partial\Omega$  adjacent to it become identified with a radial slit in the image. The two rays in  $\partial\Omega$  map to the boundary curve of a simply connected region  $\Omega'$ . See lower left in Figure 11. By the Riemann mapping theorem,  $\Omega'$  can be mapped to the upper half-plane, and the slit maps to a curved arc, meeting the real line at angle 60° (the slit looks quite straight since the tangents at the two endpoints differ by only  $\approx 2.75^{\circ}$ ).

Since the power map identifies points on the two segments adjacent to w that are equidistant from w, any equilateral triangulation of  $\Omega$  will push forward to triangulation of the upper half-plane. If the triangulation is fine enough, then all the pushed forward triangles will be nearly equilateral, except near the corners and tip of the slit. However, near the point v where the slit joins the real line, P looks like the union of a small 60°-sector and a 120°-sector and the map to P' sends each of these to subdomains of P' that contain and are contained in small sectors of the same angles. This implies the conformal maps restricted to each finite sector are approximately linear and the image of the equilateral triangulation of P' is close to equilateral in P near v. This leaves only the tip of slit. In a small neighborhood of the tip, angles are bounded above by  $72^{\circ} + \epsilon$  if the mesh is fine enough, but might exceed  $72^{\circ}$ . However, we can replace the mesh in a neighborhood of the tip by the standard mesh of a  $360^{\circ}$ -sector using Lemma 3.4. This gives the  $72^{\circ}$  bound. The construction is summarized as follows.

LEMMA 4.1. Suppose  $f: P' \to P$  is a conformal map between polygons that maps vertices to vertices. Suppose f(v') = v where v' is a vertex of P' and v is a vertex of P, with angles  $120^{\circ}$  and  $180^{\circ}$  respectively. Suppose  $\mathcal{T}$  is a nearly equilateral triangulation of P' and  $f^*\mathcal{T}$  the image triangulation. If  $\mathcal{T}$  is fine enough, then there is a neighborhood U of v and a triangulation  $\mathcal{S}$  of P that equals  $f^*\mathcal{T}$  outside V and every triangle of V touching V has all angles V is a conformal map between polygons that maps vertices to vertices. Suppose V is a vertex of V and V and V is a vertex of V and V and V is a vertex of V and V and V are vertex of V and V are vertex

### 5 The 420°-trick

In order to handle Case 2 of Theorem 1.1 we need another "trick" that can add 60° to the  $\psi$ -sum relative to the  $\theta$ -sum, but introduces triangulation angles no larger than  $\frac{5}{7} \cdot 90^{\circ} \approx 64.2857^{\circ}$ . This is precisely the angle bound we get if a 420°-vertex  $v' \in P'$  is mapped to a 360°-vertex  $v \in P$ . The 360° vertex v can occur as the end vertex of a slit in P, but how do we get a 420°-vertex in P'? We do this by considering a non-planar Riemann surface.

The idea is illustrated in Figure 13. Consider the two planar regions shown on the left side of the figure and define a Riemann surface by identifying them along the dashed ray. This creates a simply connected Riemann

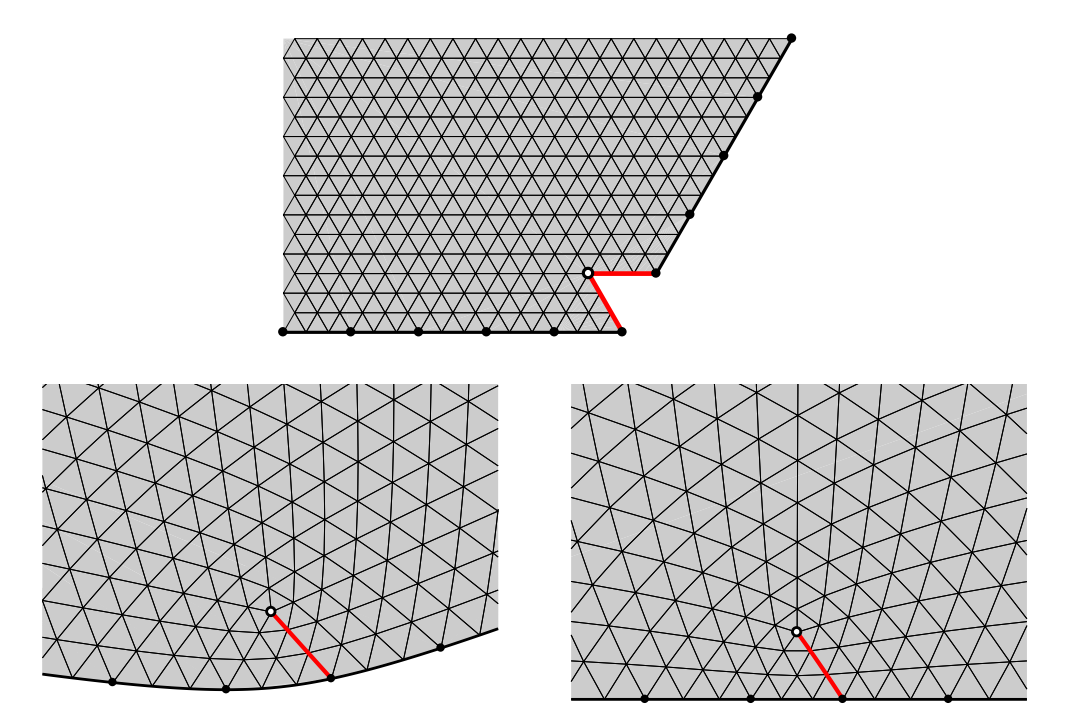
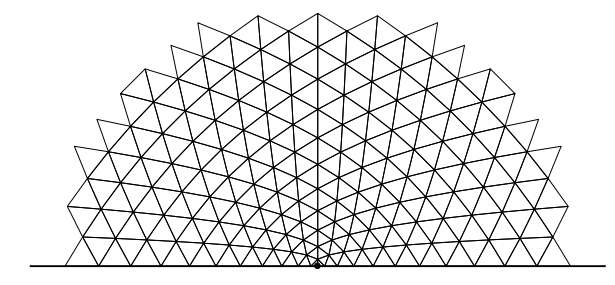


Figure 11: The cut 120-sector (top) is mapped to a simply connected region (lower left) by a branch of  $z^{6/5}$ . This is then mapped to the upper half-plane by a conformal map. Because the power map identifies points according to distance to zero (the white dot), the push forward of the triangulation is still a triangulation.

surface R with single boundary curve that is the union of two infinite rays, two finite segments and has three corners of  $60^{\circ}$ ,  $420^{\circ}$  and  $120^{\circ}$ .

We can conformally map R to a slit upper half-plane in two steps as illustrated in Figure 14 so that the two segments of  $\partial R$  that are adjacent to the 420° angle are identified with the slit, and length measure on these segments is pushed forward to the same measure on the slit. Translate the 420°-vertex to the origin and apply a branch of  $z^{6/7}$  defined on R. This maps R to a simply connected planar domain  $\Omega$  with a straight slit; the two segments of  $\partial R$  are identified with this slit in the correct way, and the two infinite rays are mapped to disjoint, unbounded arcs on  $\partial \Omega$ . The domain  $\Omega$  can then be conformally mapped to a half-plane. Thus equilateral triangulations of R will be mapped to triangulations of the upper half-plane.



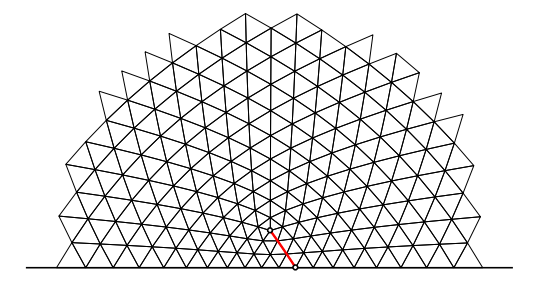


Figure 12: The left shows the equilateral triangulation of a  $120^{\circ}$ -sector pushed forward to the half-plane by  $z^{3/2}$ . The right shows the triangulation coming from the " $120^{\circ}$ -trick". These two meshes can be merged using quasiconformal interpolation as described in the text.

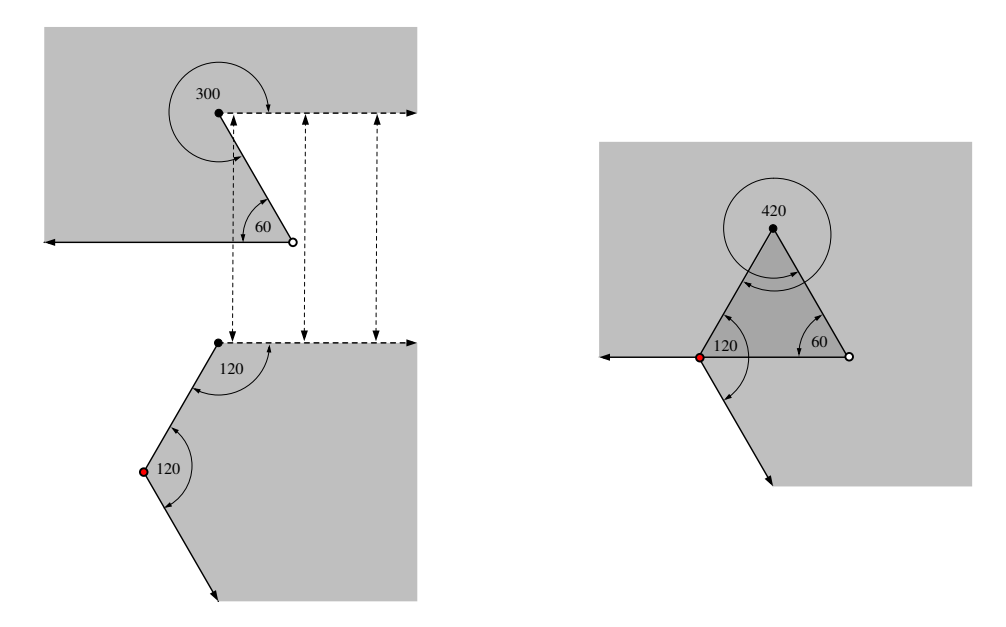


Figure 13: Here a  $180^{\circ}$  vertex in P corresponds to a  $420^{\circ}$  in P'. This is obtained by making P' a Riemann surface instead of a planar domain. The surface can be constructed from two planar domains glued along the dashed edges of each as illustrated on the left. The darker triangle indicates where the surface has two sheets over the plane.

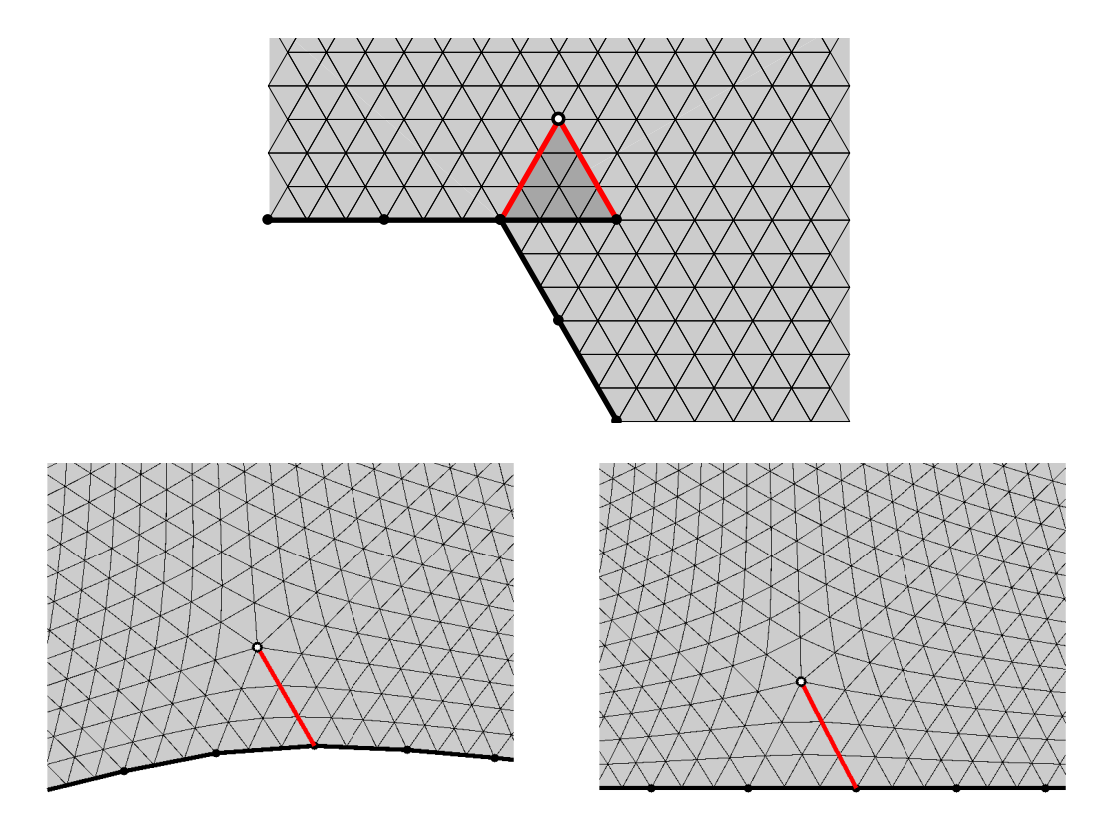


Figure 14: The Riemann surface R can be conformally mapped to a slit domain  $\Omega$  by a branch of  $z^{6/7}$ . This map is followed by a conformal map to the upper half-plane that bends the the straight slit to an analytic arc (but it looks quite straight; the tangent directions only change by about 1° along the arc).

#### 6 Sufficiency in Theorem 1.1

Necessity of the conditions in Theorem 1.1 was already sketched before the statement of the theorem, and more detailed arguments for this can be found in Gerver's paper [15] and in [7]. Here we prove the new direction of the theorem: sufficiency.

*Proof.* We want to show that any polygon P (possibly after adding extra vertices) can be conformally mapped to a 60°-polygon P', with the restrictions on the angles given by (2.2). We will use the 120°-trick to "fix" the pushed forward triangulation in a neighborhood of a few boundary points, but the 420°-trick is not needed until the proof of Cases 2 and 3 later.

The Schwarz-Christoffel formula gives a conformal map f of the disk onto a polygonal region P in terms of two types of data. First are the angles of P: suppose  $V_P = \{v_j\}_1^N$  are the vertices of P and the interior angle at  $v_j$  is  $\alpha_j \cdot 180^\circ$ . Second, suppose f maps  $z_j \in \mathbb{T}$  to  $v_j \in P$ ; these points are the conformal prevertices of P, and also called the **Schwarz-Christoffel parameters** of f. Then the conformal map f is given by

(6.3) 
$$f(z) = A + C \int_{z_j}^{z} \prod_{j=1}^{N} (1 - \frac{w}{z_j})^{\alpha_j - 1} dw,$$

for some appropriate choice of constants A, C. See e.g., [12], [22], [27]. The formula was discovered independently by Christoffel in 1867 [9] and Schwarz in 1869 [26], [25]. For other references and a brief history, see Section 1.2 of [12]. Given a polygon P, the angles are known, but the prevertices must be solved for, e.g., see [6].

Given N distinct points  $\mathbf{z} = \{z_1, \dots, z_N\}$  on the unit circle and N real values  $\{\alpha_1, \dots, \alpha_N\}$  summing to N-2, Formula (6.3) defines a locally 1-1 holomorphic function on the disk that maps each component of  $\mathbb{T} \setminus \mathbf{z}$  to a line segment, with the segments meeting at  $f(z_k)$  making interior angle  $\alpha_k \cdot 180^\circ$ . The map given by (6.3) is always locally 1-1 on  $\mathbb{D}$ , but need not be globally 1-1 in general. However, the image is always a Riemann surface with an obvious projection onto the plane. For the proof of Case 1 of Theorem 1.1 we can arrange for the image to be a planar 60°-polygon. In the proof of Case 2, given at the end of this section, the image is allowed to be a non-planar 60°-surface (this occurs when we apply the 420° trick).

Given an N-gon P, we take some conformal map f of its interior to the unit disk,  $\mathbb{D}$ . The N vertices of P map to N distinct points  $\mathbf{z}=\{z_1,\ldots,z_N\}$  on the unit circle  $\mathbb{T}$ . We then want to choose N real values  $\psi_k\in Z=\{60^\circ,120^\circ,180^\circ,240^\circ,300^\circ\}$  so that  $\sum_k\psi_k=180(N-2)$ . If this is possible, we then set  $\alpha_k=\psi_k/180$  and apply the Schwarz-Christoffel formula to get a map  $g:\mathbb{D}\to P'$ . Then  $g\circ f:P\to P'$  is the desired map. However, as noted in Sections 1 and 2, such a choice of angles  $\psi_k$  may not be possible without adding extra vertices to P.

To handle the general situation, first choose six interior points of some edge of P. This creates an M-gon with M=N+6. These are 180°-vertices in P and are assigned to have angle  $\psi_v=120^\circ$  in P'. Assign angle 180° to every other vertex of P', so the  $\psi$ -angle sum is  $6 \cdot 120^\circ + 180^\circ N = (M-2)180^\circ$ . Applying Schwarz-Christoffel gives a a 60°-hexagon, as in Figure 15.

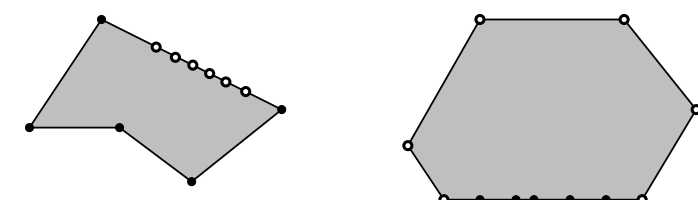


Figure 15: In the proof of Case 1 of Theorem 1.1 we can assume P' is planar. The first step is to choose six "artificial" vertices on one edge of P and make these correspond to six  $120^{\circ}$ -vertices in P'.

Next we modify the angle assignments to get a P' that approximates this hexagon. Let  $L: V_P \to \mathbb{N}$  be a  $\phi$ -admissible labeling of the vertices of P. For  $v \in V_P$ , assign angle  $60^{\circ} \cdot L(v)$  to the corresponding vertex v' of P'. In order to adjust the angle sums, for each vertex v of P we define either 0, 1 or 2 "associated vertices". The new vertices will be in the edge of P that begins with v (P has the counterclockwise orientation with the domain interior on the left) and may be taken as close to v as we wish. The vertices associated to v on P have angle 180°

and the corresponding vertices associated to v' in P' have angle either 120° or 240°. These angles are assigned so that P' leaves the last associated vertex in the same direction as it entered v'. This implies that the part of P' near v' approximates a straight line. The rules for making the assignments are simple and illustrated in Figure 16. Suppose v is an original vertex of P with interior angle  $\theta_v$ :

- i. if  $0 < \theta \le 72^{\circ}$ , set  $\psi_v = 60^{\circ}$  and add two vertices each with angle 240°,
- ii. if  $72^{\circ} < \theta \le 144^{\circ}$ , set  $\psi_v = 120^{\circ}$  and add one vertex with angle 240°,
- iii. if  $144^{\circ} < \theta \le 216^{\circ}$ , set  $\psi_v = 180^{\circ}$  and add no associated vertices,
- iv. if  $216^{\circ} < \theta \le 288^{\circ}$ , set  $\psi_v = 240^{\circ}$  and add one vertex with angle  $120^{\circ}$ ,
- v. if  $288^{\circ} < \theta \le 360^{\circ}$ , set  $\psi_v = 300^{\circ}$  and add two vertices of angle 120°.

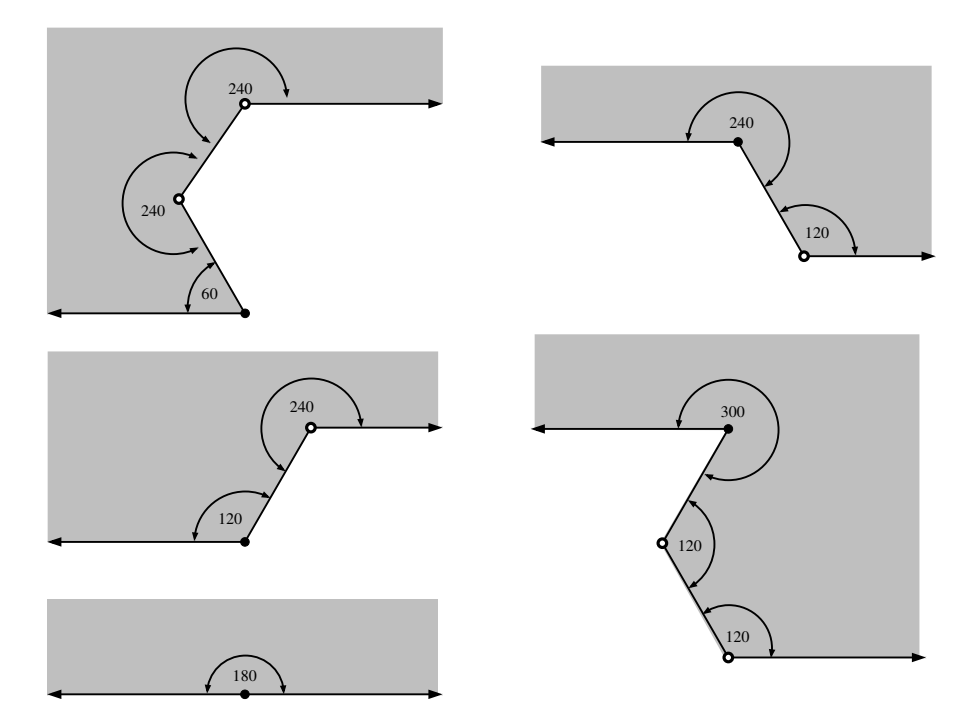


Figure 16: The five cases for assigning image angles and associated vertices. In each case the black indicates the image of the original vertex and the white dots the new associated vertices. These arcs illustrate small subarcs of the  $60^{\circ}$ -polygon P'. The associated vertices map to  $180^{\circ}$  vertices that we add to the edges of P.

If the vertices associated to v are close enough to v, then the image arc is close to a line. See Figure 17. In particular, P' is not self-intersecting and so is a  $60^{\circ}$ -polygon. By Lemma 3.5, P' has nearly equilateral triangulations. In the remainder of the proof we will take this triangulation as fine as is needed (but only finitely many conditions are involved, so we finish with a positive grid size).

Each original vertex with angle  $\theta_v \geq 36^\circ$  was assigned an image angle  $\psi_v$  in the allowable range from (2.2). Thus transferring a nearly equilateral triangulation of P' gives a triangulation of P with all angles between  $36^\circ$  and  $72^\circ$  except possibly in small neighborhoods of these vertices, where the angle bounds are with all angles between  $36^\circ - \epsilon$  and  $72^\circ + \epsilon$ , and  $\epsilon$  can be made as small as we wish be taking the triangulation fine enough. In a neighborhood of each such vertex, we may use Lemma 3.7 to replace the pushed forward triangulation with a sector triangulation for which the bounds  $36^\circ, 72^\circ$  hold.

For each original vertex with interior angle  $\theta_v < 36^\circ$  the same argument applies, except that now we get the bounds in the interval  $I(\theta_v) = [\theta_v, 90^\circ - \theta_v/2]$ . Again, we may use interpolation to locally replace the pulled back triangulation (which might only approach the desired bounds as the triangulation gets finer), with a sector triangulation attaining the desired bounds.

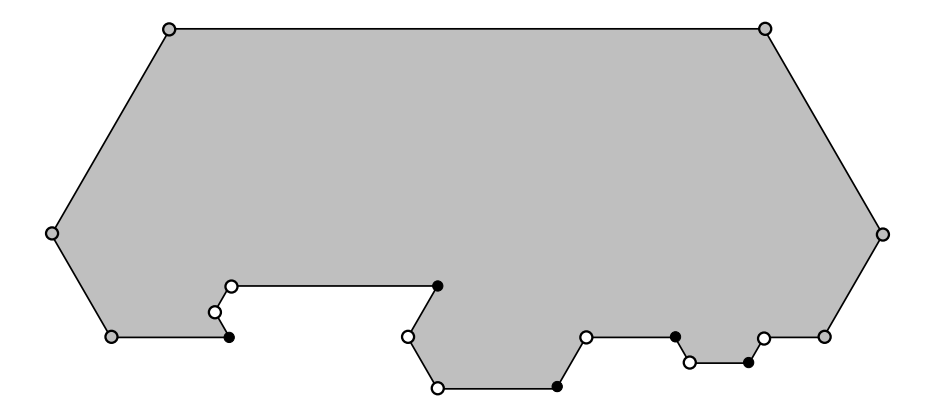


Figure 17: The  $60^{\circ}$ -polygon P'. The six gray points were added at the beginning, the black points are the images of the original vertices and the white points are the associated vertices.

Next consider the associated vertices with angles  $> 120^{\circ}$ ; Cases (i) and (ii) above. In Case (i) each  $240^{\circ}$ -vertex is hit by 4 equilateral triangles and so each  $60^{\circ}$  sub-angle is mapped to an angle of size  $180^{\circ}/4 = 45^{\circ}$ . In this case, the interpolation with a sector triangulation isn't needed; with small enough distortion, the angles are already inside  $[36^{\circ}, 72^{\circ}]$ . Case (ii) is the same, except there is only one associated vertex.

Finally we consider Cases (iv) and (v). Here we only use image angles of size 120°. Such an angle is divided into two 60° angles that are mapped to 90° by the conformal map. These angles are too large for our purposes, so to fix this we use Lemma 4.1 to interpolate between the conformal image triangulation and the triangulation of the half-plane coming from the 120°-trick. This gives a triangulation of with angles in  $I(36^\circ) = [36^\circ, 72^\circ]$  in a neighborhood of each associated vertex. This completes the proof of Case 1 of Theorem 1.1.

Now we turn to Cases 2 and 3. We have to modify the construction in the proof of Case 1 to avoid using the  $120^{\circ}$ -trick in Case 2 (this forces an angle  $\geq 72^{\circ}$ ), and to avoid both the  $120^{\circ}$ -trick and the  $420^{\circ}$ -trick in Case 3 (the latter forces angles  $\geq \frac{5}{7} \cdot 90^{\circ}$ ).

Suppose L is a  $\phi$ -admissible labeling of  $V_P$  so that  $\kappa(\phi) = \kappa(L)$  (i.e., choose L to minimize  $|\kappa(L)|$  among admissible labelings). As before, let  $\theta_v$  denote the angle of P at vertex v, and for each vertex v in P, suppose  $\psi_v = L(v) \cdot 60^\circ$  is the tentative corresponding angle of v' in P'. As we have noted before,

$$\sum_{v} \theta_{v} = (|V_{P}| - 2)180^{\circ} = 60^{\circ} (3|V_{P}| - 6)$$

$$= 60^{\circ} \left( 3|V_{P}| - 6 - \sum_{v} L(v) + \sum_{v} L(v) \right) = 60^{\circ} \cdot \kappa(L) + \sum_{v} \psi_{v}.$$

Thus in Case 2 ( $\kappa(L) \leq 0$ ) we only need to introduce 180°-vertices on P that correspond to 240°-vertices in P'. If  $\phi \geq 67.5^{\circ}$ , we can do this by replacing the pushed forward triangulation from P' by the 240°-sector triangulation. If  $\frac{5}{7} \cdot 90^{\circ} \leq \phi < 67.5^{\circ}$  then we replace it with the triangulation of the half-plane obtained by the 420°-trick. This proves sufficiency in Case 2.

Finally, if  $\kappa(L) = 0$ , then no extra vertices or "tricks" are needed. We simply use a fine enough triangulation pushed forward by the conformal map from P' to P and replace it in a neighborhood of each vertex by the appropriate sector mesh. This completes the proof in Case 3.

## References

- [1] L. V. Ahlfors. Lectures on quasiconformal mappings. The Wadsworth & Brooks/Cole Mathematics Series. Wadsworth & Brooks/Cole Advanced Books & Software, Monterey, CA, 1987. With the assistance of Clifford J. Earle, Jr., Reprint of the 1966 original.
- [2] B.S. Baker, E. Grosse, and C.S. Rafferty. Nonobtuse triangulation of polygons. *Discrete Comput. Geom.*, 3(2):147–168, 1988.

- [3] M. Bern, H. Edelsbrunner, D. Eppstein, S. Mitchell, and T. S. Tan. Edge insertion for optimal triangulations. In LATIN '92 (São Paulo, 1992), volume 583 of Lecture Notes in Comput. Sci., pages 46–60. Springer, Berlin, 1992.
- [4] M. Bern and D. Eppstein. Mesh generation and optimal triangulation. In *Computing in Euclidean geometry*, volume 1 of *Lecture Notes Ser. Comput.*, pages 23–90. World Sci. Publ., River Edge, NJ, 1992.
- [5] C. J. Bishop. Conformal welding and Koebe's theorem. Ann. of Math. (2), 166(3):613–656, 2007.
- [6] C.J. Bishop. Conformal mapping in linear time. Discrete Comput. Geom., 44(2):330–428, 2010.
- [7] C.J. Bishop. Optimal angle bounds for polygonal triangulation. 2021. Preprint.
- [8] Yu. D. Burago and V. A. Zalgaller. Polyhedral embedding of a net. Vestnik Leningrad. Univ., 15(7):66–80, 1960.
- [9] E.B. Christoffel. Sul problema della tempurature stazonaire e la rappresetazione di una data superficie. Ann. Mat. Pura Appl. Serie II, pages 89–103, 1867.
- [10] H.T. Croft, K.J. Falconer, and R.K. Guy. Unsolved problems in geometry. Problem Books in Mathematics. Springer-Verlag, New York, 1991.
- [11] T.A Driscoll. Algorithm 843: Improvements to the Schwarz-Christoffel Toolbox for MATLAB. ACM Transactions on Mathematical Software (TOMS), 31(2):239–251, 2005.
- [12] T.A. Driscoll and L.N. Trefethen. Schwarz-Christoffel mapping, volume 8 of Cambridge Monographs on Applied and Computational Mathematics. Cambridge University Press, Cambridge, 2002.
- [13] H. Edelsbrunner, T.S. Tan, and R. Waupotitsch. An  $O(n^2 \log n)$  time algorithm for the minmax angle triangulation. SIAM J. Sci. Statist. Comput., 13(4):994–1008, 1992.
- [14] D. Eppstein. Acute square triangulation. Webpage https://www.ics.uci.edu/eppstein/junkyard/acute-square/, Accessed: January 2, 2021.
- [15] J. L. Gerver. The dissection of a polygon into nearly equilateral triangles. Geom. Dedicata, 16(1):93–106, 1984.
- [16] D. H. Hamilton. Conformal welding. In *Handbook of complex analysis: geometric function theory, Vol. 1*, pages 137–146. North-Holland, Amsterdam, 2002.
- [17] C.L. Lawson. Software for  $C^1$  surface interpolation, pages ix+388. Academic Press [Harcourt Brace Jovanovich Publishers], New York, 1977. Publication of the Mathematics Research Center, No. 39.
- [18] D. T. Lee and A. K. Lin. Generalized Delaunay triangulation for planar graphs. Discrete Comput. Geom., 1(3):201–217, 1986.
- [19] O. Lehto and K. I. Virtanen. Quasiconformal mappings in the plane. Springer-Verlag, New York-Heidelberg, second edition, 1973. Translated from the German by K. W. Lucas, Die Grundlehren der mathematischen Wissenschaften, Band 126.
- [20] H. Maehara. Acute triangulations of polygons. European J. Combin., 23(1):45-55, 2002.
- [21] S.A. Mitchell. Approximating the maxmin-angle covering triangulation. volume 7, pages 93–111. 1997. Fifth Canadian Conference on Computational Geometry (Waterloo, ON, 1993).
- [22] Z. Nehari. Conformal mapping. Dover Publications Inc., New York, 1975. Reprinting of the 1952 edition.
- [23] S. Rohde. On conformal welding and quasicircles. Michigan Math. J., 38:111-116, 1991.
- [24] S. Saraf. Acute and nonobtuse triangulations of polyhedral surfaces. European J. Combin., 30(4):833–840, 2009.
- [25] H.A. Schwarz. Confome abbildung der oberfläche eines tetraeders auf die oberfläche einer kugel. *J. Reine Ange. Math.*, pages 121–136, 1869. Also in collected works, [26], pp. 84-101.
- [26] H.A. Schwarz. Gesammelte Mathematische Abhandlungen. Springer, Berlin, 1890.
- [27] L. N. Trefethen and T.A. Driscoll. Schwarz-Christoffel mapping in the computer era. In Proceedings of the International Congress of Mathematicians, Vol. III (Berlin, 1998), number Extra Vol. III, pages 533–542 (electronic), 1998.
- [28] L.N. Trefethen. Numerical computation of the Schwarz-Christoffel transformation. SIAM J. Sci. Statist. Comput., 1(1):82–102, 1980.
- [29] L. Yuan. Acute triangulations of polygons. Discrete Comput. Geom., 34(4):697–706, 2005.
  - C.J. Bishop, Dept. of Math., Stony Brook University, Stony Brook NY 11794-3651 bishop@math.stonybrook.edu